

11-5  
11-186  
11-186

# Application of Response Surface Techniques to Helicopter Rotor Blade Optimization Procedure

1-18

Joseph Lynn Henderson  
Virginia Polytechnic Institute and State University  
Blacksburg, Virginia

Joanne L. Walsh and Katherine C. Young  
NASA Langley Research Center  
Hampton, Virginia

(NASA-TM-111274) APPLICATION OF  
RESPONSE SURFACE TECHNIQUES TO  
HELICOPTER ROTOR BLADE OPTIMIZATION  
PROCEDURE (NASA Langley Research  
Center) 18 p

N96-18505

Unclas

G3/05 0099873

Presented at  
AHS National Technical Specialist' Meeting  
Rotorcraft Structures: Design Challenges and Innovative Solutions  
Williamsburg, Virginia  
October 30 - November 2, 1995

1  
)

# **Application Of Response Surface Techniques To Helicopter Rotor Blade Optimization Procedure**

Joseph L. Henderson  
Virginia Polytechnic Institute and State University

Joanne L. Walsh, and Katherine C. Young  
NASA Langley Research Center

## **Abstract**

In multidisciplinary optimization problems, response surface techniques can be used to replace the complex analyses that define the objective function and/or constraints with simple functions, typically polynomials. In this work a response surface is applied to the design optimization of a helicopter rotor blade. In previous work, this problem has been formulated with a multilevel approach. Here, the response surface takes advantage of this decomposition and is used to replace the lower level, a structural optimization of the blade. Problems that were encountered and important considerations in applying the response surface are discussed. Preliminary results are also presented that illustrate the benefits of using the response surface.

## **Introduction**

In dealing with multidisciplinary design optimization (MDO), several problems arise. The analysis codes of the various disciplines are vastly different and difficult to integrate. In addition, these analyses must be linked to an optimizer, which is another difficult task. Because of their complexity, multidisciplinary problems are typically decomposed into several simpler subproblems. This process is known as multilevel decomposition (Refs. 1-6), and the functions that pass information between the various levels may not always be smooth. Moreover, individual disciplines may require more than one computational model. For example, the finite-element structural analysis may employ a simplified aerodynamic code to predict the loads, and the Computational Fluid Dynamics (CFD) analysis may use a simplified structural model such as the weight equation. Researchers are investigating approximation concepts to reduce the high computational costs associated with MDO problems. Barthelemy (Ref. 7) reviews some of the most recent approximation concepts used in structural optimization problems. As discussed in Ref. 7, one area which is gaining attention is response surface methodology (e.g., Refs. 7-15).

A response surface is a means of approximating complex functions and/or analyses with a polynomial function or a neural network. Response surfaces will be discussed in more detail later in this paper. The benefits of a response surface approach to MDO are three-fold. First, the response surface provides a method for smoothing the noisy functions (Refs. 7 and 8). Eason and Fenton (Ref. 9) suggest that many complex engineering analyses (e.g., finite-element models) yield nonsmooth functions that may cause errors in the finite difference derivative calculations commonly used in conventional optimization algorithms. Thus, these analyses should be replaced with smooth analytical functions. Second, the response surface approximation provides one discipline with a quick assessment of other disciplinary analyses, similar to empirical structural weight equations. Third, response surfaces are amenable to parallel computation, whereby the various disciplinary analyses can be conducted on different processors or even different machines (Ref. 7).

References 7–14 describe applications where response surfaces have been used in structural optimization problems. In these applications, response surfaces are generated to develop analytical functions in place of the complex analyses or experimental data. These analytical functions are then used in the optimization procedure. The work presented in this paper applies response surface methodology to a rotor blade optimization procedure (Ref. 16) which used multilevel decomposition. Unlike the applications in Refs. 8–14, a response surface is generated to approximate an entire optimization procedure. Specifically, the lower level structural optimization in Ref. 16 is replaced by a response surface. First, a summary of the multilevel rotor blade optimization procedure (Ref. 16) is given. Next, a discussion of response surface implementation is discussed. Finally, results are presented.

### **Integrated Aerodynamic/Dynamic/Structural (IADS) Optimization Procedure**

Reference 16 describes an integrated aerodynamic/dynamic/structural (IADS) optimization procedure for helicopter rotor blades. The procedure combines performance, dynamics, and structural analyses with a general purpose optimizer (CONMIN, Ref. 17) using multilevel decomposition techniques. The upper level optimizes the blade by changing global quantities such as blade planform, twist, and stiffness distributions. The upper level chord and stiffness distributions are treated as independent quantities. The reconciliation between these distributions is done on the lower level, which consists of several independent subproblems at stations along the blade radius. These subproblems optimize detailed cross-sectional dimensions to assure structural integrity of the blade and to reconcile the upper level independent chord and stiffness distributions with the lower level calculated stiffness distributions. This reconciliation is improved further by a set of upper level coordination constraints.

#### **Upper Level Optimization**

For the present work, the blade is assumed to have a rectangular planform and constant stiffnesses spanwise. Thus, a subset of the upper level design variables described in Ref. 16 is used. These design variables (Fig. 1) are the maximum pretwist  $\theta_{tw}$ , the root chord  $c_r$ , and the four blade stiffnesses: chordwise bending  $E_{xx}$ , flapwise bending  $EI_{zz}$ , extensional  $EA$ , and torsional  $GJ$  stiffness.

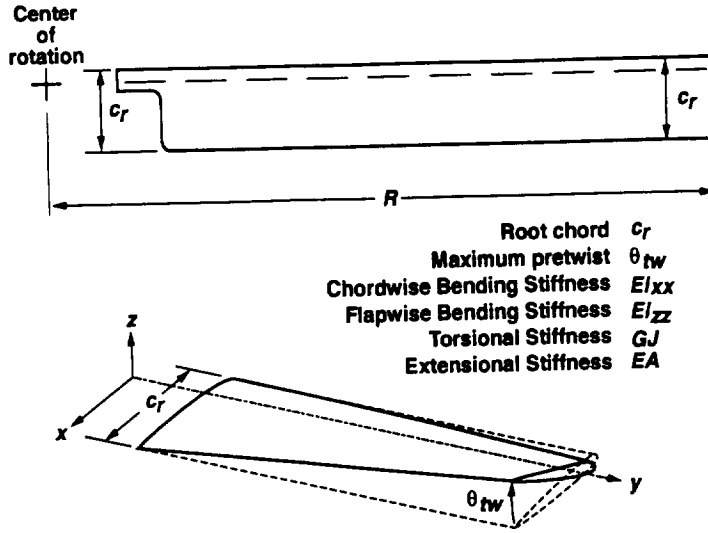


Figure 1. Upper level design variables.

The upper level objective function to be minimized is a measure of the horsepowers required in each of three flight conditions (hover, forward flight, and maneuver) and the hub shear (i.e., vibration) and is given by

$$OBJ = k_1 \frac{P_h}{P_{h_{ref}}} + k_2 \frac{P_{ff}}{P_{ff_{ref}}} + k_3 \frac{P_m}{P_{m_{ref}}} + k_4 \frac{S_{N_{ff}}}{S_{N_{ref}}} \quad (1)$$

where  $P_h$ ,  $P_{ff}$ , and  $P_m$  are the powers required in hover, forward flight, and maneuver, respectively.  $N$  is the number of blades and  $S_{N_{ff}}$  is the  $N$  per rev rotating vertical hub shear in forward flight. The terms  $k_1$ ,  $k_2$ ,  $k_3$ , and  $k_4$  are weighting factors chosen by the user.  $P_{h_{ref}}$ ,  $P_{ff_{ref}}$ ,  $P_{m_{ref}}$ , and  $S_{N_{ref}}$  are reference values used to normalize and nondimensionalize the objective function components. The constraints on the problem are aerodynamic and dynamic in nature (see Ref. 16 for details). The coordination constraint which is the means of communication between the upper and lower levels is also imposed at the upper level. The Langley-developed hover analysis HOVT (a strip-theory momentum analysis based on Ref. 18) is used to predict the power required in hover. The comprehensive rotor analysis CAMRAD/JA (Ref. 19) is used to predict forward flight and maneuver performance.

### Lower Level Optimization

The purpose of the lower level is to assess whether a structure at a given radial location can be sized to provide the stiffnesses required by the upper level optimization and still have the strength to withstand

loads calculated by the upper level analysis. In the present work a single cross section is optimized. The lower level represents the structural properties of the blade in terms of wall thickness

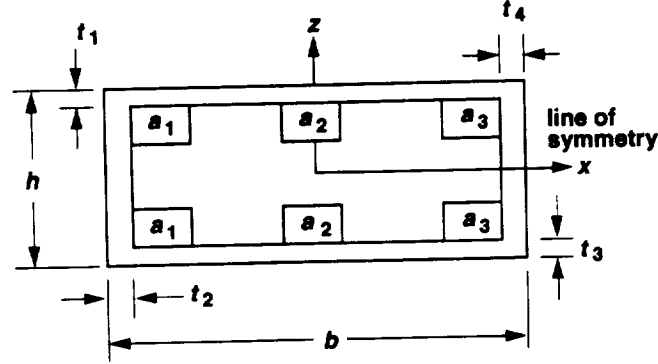


Figure 2. Lower level design variables.

and lumped areas in the box beam cross section (Fig. 2). The lower level objective function to minimized is given by

$$F = \left( \frac{EI_{zz}^L - EI_{zz}^U}{EI_{zz}^U} \right)^2 + \left( \frac{EI_{xx}^L - EI_{xx}^U}{EI_{xx}^U} \right)^2 + \left( \frac{GJ^L - GJ^U}{GJ^U} \right)^2 \quad (2)$$

and is a measure of the stiffness matching. The stiffness matching is the difference between the stiffnesses that are desired by the upper level (denoted by the superscript U) and the stiffnesses that can be obtained by the lower level (denoted by the superscript L). Constraints at the lower level assure structural integrity of the blade (see Ref. 16). For convenience, the set of lower level constraints is replaced by a single cumulative constraint, an envelope function known as the Kreisselmeir-Steinhauser (KS function, Ref. 20) function which approximates the active constraint boundary

$$KS = g_{\max} + \frac{1}{\rho} \ln \left[ \sum_{j=1}^{N_c} e^{\rho(g_{c_j} - g_{\max})} \right] \leq 0 \quad (3)$$

where  $g_{\max}$  is the maximum constraint component,  $nc$  is the number of lower level constraint components and  $\rho$  is defined by the user. The lower level optimization is repeated for various values of  $\rho$ . Initially  $\rho$  is small and then increases until a maximum value  $\rho_{\max}$  is reached. For large values of  $\rho$ ,

the value of KS approaches  $g_{\max}$ . The KS function is a single measure of the degree of constraint satisfaction or violation and is positive (violated) if at least one of the constraints  $g_{c_j}$  is violated.

### Coordination

The coordination between upper and lower levels is implemented by an upper level constraint imposed to encourage changes in the upper level design variables which promote consistency between the upper and lower level stiffnesses. Specifically, this constraint has the form

$$g = F^U - (1 + \epsilon)F_{\text{opt}}^L \leq 0 \quad (4)$$

where  $F_{\text{opt}}^L$  is the most recent value of the lower level objective function (i.e., optimum value of equation 2),  $F^U$  is an estimate of the change in  $F_{\text{opt}}^L$  caused by a change in the upper level design variable values, and  $\epsilon$  is a specified tolerance denoting the coordination parameter. The coordination constraint relays to the upper level the value of the lower level optimal objective function (i.e., how well the stiffnesses match) and how that value will change when an upper level design variable changes.

Figure 3 shows a flowchart of the optimization procedure. In this research, the entire lower level structural optimization is replaced by a response surface. The surface is generated outside the optimization cycle loop and is used both in place of the lower level during the optimization process and in the coordination constraint. The implementation of the response surface in this problem will be discussed later.

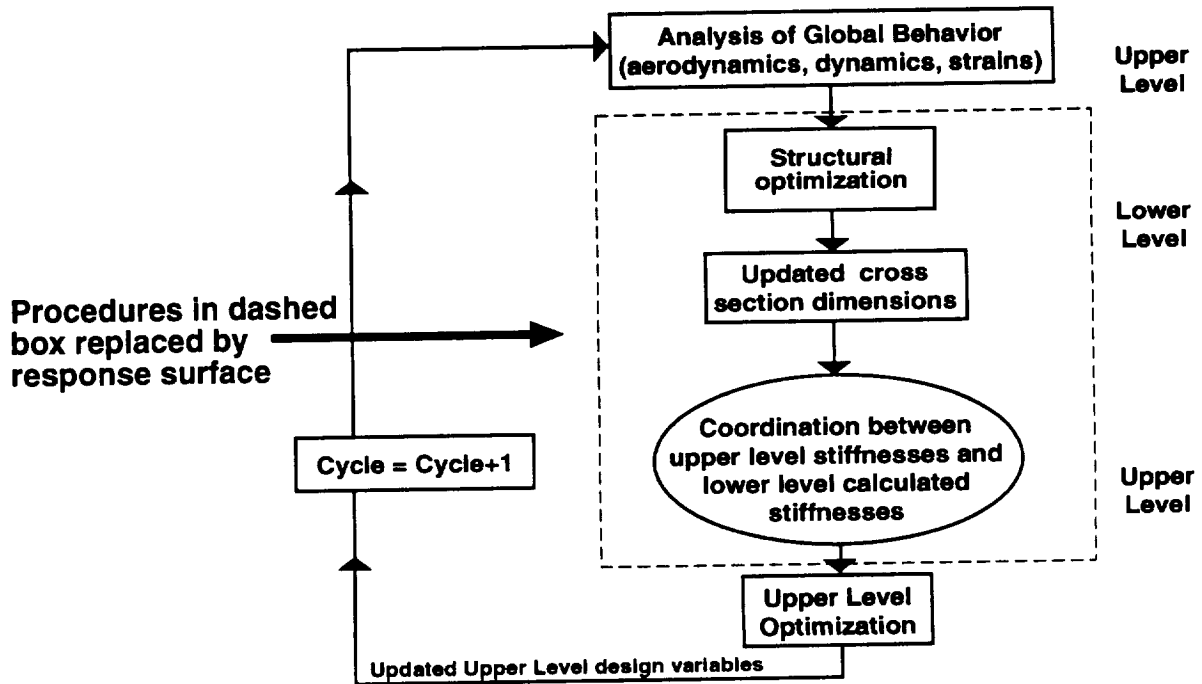


Figure 3. Flowchart of IADS optimization with response surface formulation.

## Response Surface

As previously mentioned, the response surface is an approximation that replaces the objective function and/or constraints with a polynomial expression or a neural network. The reader is referred to Refs. 7 and 15 for more details on response surface methodology. A response surface was constructed to replace the *entire lower level structural optimization procedure* in the form of the *optimum* lower level objective function ( $F_{\text{opt}}^L$ ). Therefore, the response surface predicts the stiffness mismatch between the upper and lower levels. A quadratic polynomial of the form

$$\hat{F}_{\text{opt}}^L = b_0 + \sum_{i=1}^n b_i x_i + \sum_{i=1}^n \sum_{j=i}^n b_{ij} x_i x_j \quad (5)$$

was selected as the model. Here, the coefficients  $b$  are computed by a least-squares regression analysis. The response surface is a function of the upper level design variables  $x_i$ . In this case, 6 design variables yield 28 undetermined coefficients for which to solve. The points in the design space used to generate the response surface are given by statistical experimental design (specifically, a central composite design). Figure 4 shows a central composite design in three dimensions. A set of baseline design variables (i.e., an initial guess for the optimizer) is scaled to the point  $(0, 0, 0, 0, 0, 0)$ . The baseline design variables are perturbed by  $\pm 10$  percent. Several larger percentages (e.g.,  $\pm 25$ ) were tried. The CAMRAD/JA analysis experienced numerical difficulties in analyzing some of the design points generated with larger perturbation values. For the work presented here, the  $\pm 10$  percent was found to be the best value. The design variables are then scaled to  $\pm 1$ . These points form the vertices of the hypercube. Finally, the centers of each face of the hypercube are selected. The 6 design variables in this problem used 77 design points, which creates an overdetermined system.

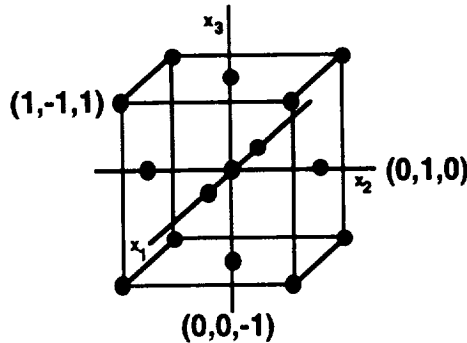


Figure 4. Central composite design in three dimensions.

## Important Considerations

### Response Surface Implementation

In conducting this research, several important considerations must be addressed in the application of a response surface to this type of problem, in which an entire optimization is replaced with a



polynomial function. First one must determine what the response surface will approximate; two possible choices are the optimal lower level objective function value ( $F_{opt}^L$ ) or the same objective penalized by the lower level constraints ( $F_{opt}^L + \text{penalty} \cdot \text{KS function}$ ). A third possibility that was not explored is to build a second response surface for the lower level KS function constraint and use this approximation as an additional upper level constraint. Introduction of the constraints from the lower level ensures that the designs are feasible; however, for the results presented here feasibility was not a concern because the lower level constraints of the generated designs were satisfied. Therefore, the unpenalized optimal lower level objective function was selected to be approximated by the response surface.

### Coordination Constraint

The second consideration that requires attention is the selection of the coordination constraint. Recall that the coordination constraint is the means by which the upper and lower levels communicate. In essence, the coordination constraint discourages the upper level optimization from degrading the stiffness matching achieved on the lower level. As formulated in Ref. 16, the lower level provides the upper level not only with  $F_{opt}^L$ , but also with the optimal values of the lower level design.  $F^U$  in eqn. 4, is evaluated at the upper level using the current upper level design variable values and the previous optimum lower level design variables.  $F_{opt}^L$  is the previous optimum lower level objective function. When a response surface formulation is used, however, all dependence on lower level design variables is lost; the values of the lower level design variables are not available. The approximating polynomial is only a function of the upper level design variables. One possible solution to this problem is to build a response surface for each of the six lower level design variables, as well as for the lower level optimization. Another solution is to reformulate the coordination constraint as follows

$$g = F_{opt}^L \leq \gamma \quad (\gamma = 0.001) \quad (6)$$

This constraint forces the matching of stiffnesses to be within a small tolerance ( $\gamma$ ) of zero. Now the coordination constraint can be evaluated by the response surface (eqn. 5).

### Quality of Design Points Used to Generate the Response Surface

The third issue that must be examined is whether or not the response surface represents an *optimum* design. In the present work, the response surface is formulated as a quadratic approximation of  $F_{opt}^L$ . The coefficients of this polynomial are determined from the 77 structural optimizations used to generate the response surface. Therefore, the response surface approximation is only as good as those 77 design points. If those designs are not optimal, then the response surface will be ineffective in predicting the stiffness mismatch (its desired task). Below is a situation encountered in this study where optimality of individual points was a problem.

Initially, the response surface was generated from a set of 77 optimum lower level designs. Each design was obtained using the same minimum and maximum values for  $p$  in the KS function (Eqn. 3)

used in Ref. 16. When the structural optimization at the lower level was replaced with this response surface, the upper level (overall) optimization consistently converged to the set of baseline design variables given as an initial guess, which was not an optimum. To assess the problem, the generation of the response surface data points was examined. The lower level structural optimization was performed with different initial values of wall thicknesses. (Note: initially the lumped areas are set to zero.) Each time the initial thickness values were changed, the lower level objective function converged to a different value  $F_{\text{opt}}^L$ . These different values suggest the possibility of many local optima in the lower level objective function. However, this possibility was discovered not to be the case; a test was conducted in which the objective function was evaluated at regular intervals between two “optimum” points ( $\mathbf{x}_1$  and  $\mathbf{x}_2$ ). These intermediate points were governed by a parameter  $\alpha$  ( $0 \leq \alpha \leq 1$ ) in the following expression:

$$\mathbf{x} = \alpha \mathbf{x}_1 + (1 - \alpha) \mathbf{x}_2 \quad (7)$$

Several pairs of points were tested; a sample of the results is presented in Fig. 5. This plot shows that the lower level objective function does not experience any local maxima or minima.

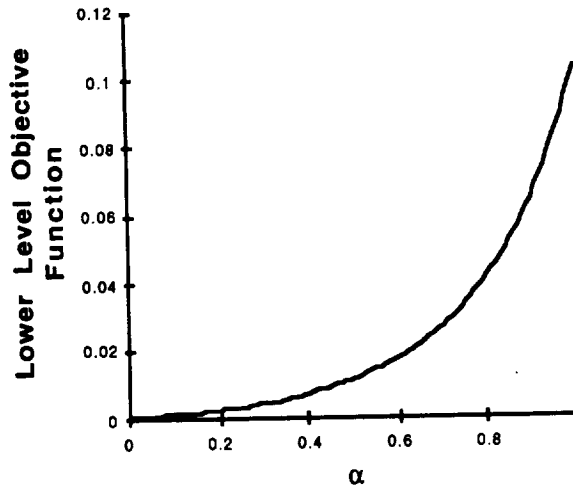


**Figure 5. Test for local optima in lower level objective function.**

Next the maximum value for  $\rho$  was increased. Then the structural optimizations at the lower level for all initial thicknesses yielded the same lower level optimum. The response surface was then regenerated with 77 new structural optimizations and the overall optimization no longer converged to the set of baseline design variables. The reason that a global optimum was not found was attributed to the value of  $\rho$  in the KS function (Eq. (3)). The maximum  $\rho$  value was too small; thus, the structural optimization converged prematurely. This response surface was used to compute the results presented in this paper.

### Quality of Fit

Lastly, once the response surface has been generated, the quality of the fit must be assessed. Two approaches were considered for this assessment. The first approach is to measure the percent error between the response surface and the actual structural optimization

$$\% \text{ error} = 100 \cdot \left| \frac{\hat{F}_{\text{opt}}^L - F_{\text{opt}}^L}{F_{\text{opt}}^L} \right| \quad (8)$$

A measure of the error is possible at individual points in the design space. However, as discussed earlier, many multilevel functions can be noisy which is illustrated by Fig. 6. Thus, although individual points may not be close to the response surface values, the overall fit of the response surface could be adequate. Carpenter (Ref. 14) suggests a nondimensional root mean square (RMS) error as a measure of this overall fit

$$\text{RMS error} = 100 \cdot \frac{\sqrt{\frac{\sum_{i=1}^N (F_{\text{opt},i}^L - \hat{F}_{\text{opt},i}^L)^2}{N}}}{\bar{F}_{\text{opt}}^L} \quad (9)$$

Here,  $\bar{F}_{\text{opt}}^L$  is the average value of the optimal lower level objective function over  $N$  points examined;  $\bar{F}_{\text{opt}}^L$  is given by

$$\bar{F}_{\text{opt}}^L = \frac{\sum_{i=1}^N F_{\text{opt}}^L}{N} \quad (10)$$

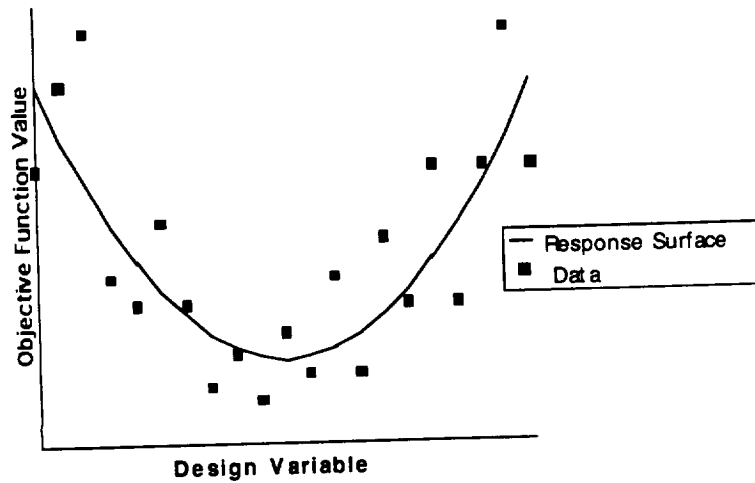


Figure 6. Response surface approximation.

The RMS error computed for the set of 77 points used to generate the response surface was 18 percent. The least-squares regression analysis that computes the coefficients of the approximating polynomial seeks to minimize error at these points. A better test of the quality of fit, therefore, is to compute the RMS error at 50 random points in the design space; this value was 59 percent. Both errors are reasonable and are comparable to the results reported by Carpenter (Ref. 14). A total of 127 points were used to generate and validate the response surface.

## Results

Both the response surface formulation and the IADS formulation with the modified coordination constraint (Eq. (6)) were studied. Both optimization routines were implemented on the NASA Langley Cray 2 supercomputer. Results are presented using the parameters in Table 1. Table 2 presents the upper level design variables and objective function for the initial blade design. The upper level objective function OBJ is also given in the table. This design is infeasible because an upper level frequency constraint is violated. Neither formulation was run to convergence. Results are presented after 15 cycles and 30 cycles. The response surface was only generated once.

Table 1. Parameters

N, number of blades	4
$k_1$	10.0
$k_2$	5.0
$k_3$	5.0
$k_4$	0.5
$P_{h_{ref}}$	15 hp
$P_{ff_{ref}}$	13 hp
$P_{m_{ref}}$	12 hp
$S_{4_{ref}}$	2 lbf

Table 2. Initial Guess for Blade Design

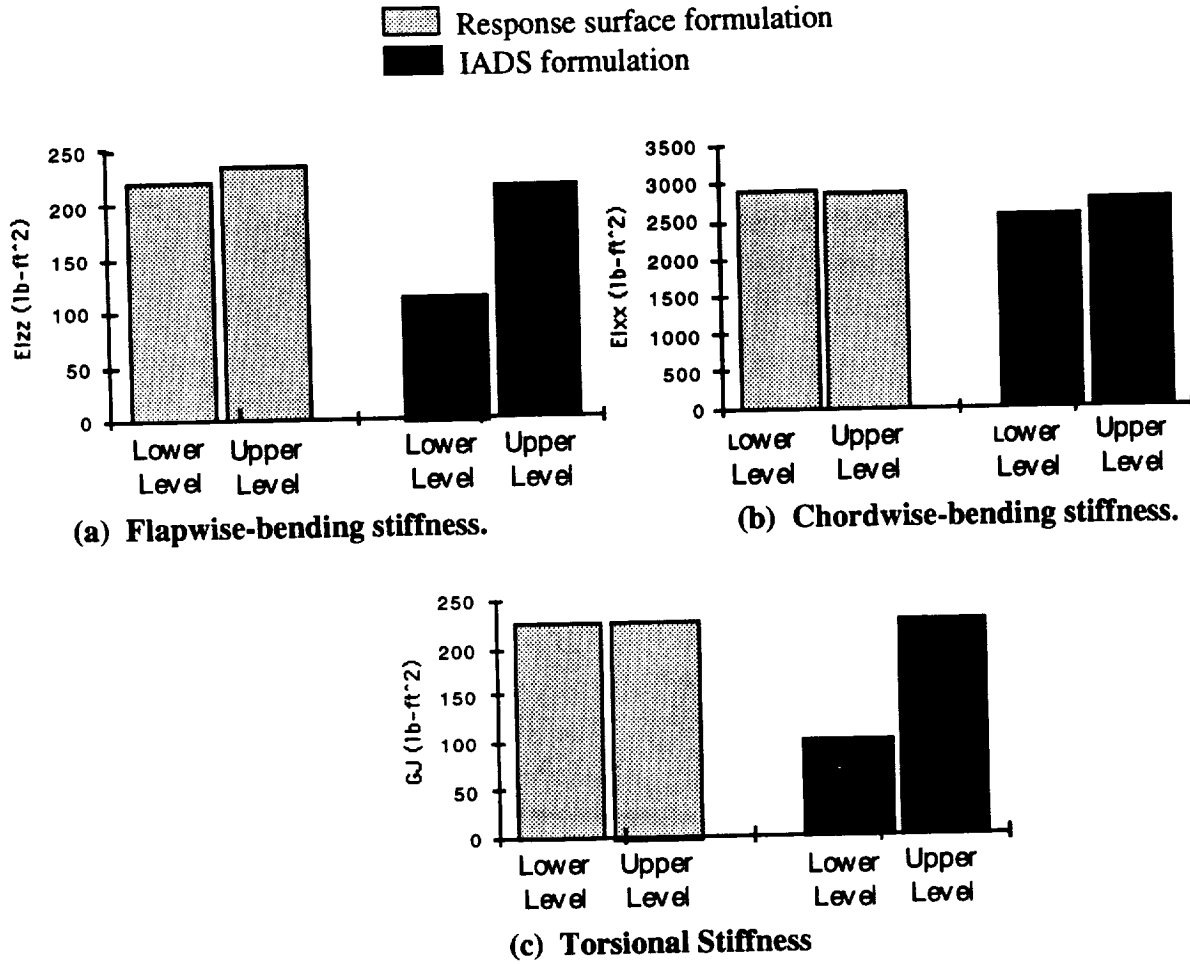
Upper Level Design Variable	Initial Design
Twist (deg)	-9.00
Chord (ft)	0.4500
$EI_{xx}$ (lb-ft <sup>2</sup> )	2,907
$EI_{zz}$ (lb-ft <sup>2</sup> )	226.6
GJ (lb-ft <sup>2</sup> )	261.9
EA (lb)	1,466,000
OBJ	20.89

Table 3 compares the results of the two formulations after 15 optimization cycles. In both cases, the value of OBJ has decreased from the initial value. The design variable values are similar, except for the chord value. At first glance, the IADS formulation seems to perform better than the response surface. However, one also needs to examine what is happening at the lower level (i.e., the stiffness matching). Recall with the response surface formulation, the actual wall thicknesses and lumped areas are not available. To determine these dimensions and to assure the structural integrity of the response surface generated blade design, an lower level structural optimization was performed at the lower level to determine how well the stiffnesses match.

Table 3. Optimization Results after 15 Cycles

Upper Level Design Variable	Response Surface	IADS
Twist (deg)	-12.10	-12.55
Chord (ft)	0.4381	0.3553
El <sub>xx</sub> (lb-ft <sup>2</sup> )	2,831	2,731
El <sub>zz</sub> (lb-ft <sup>2</sup> )	231.9	212.5
GJ (lb-ft <sup>2</sup> )	225.4	225.0
EA (lb)	1,469,000	1,471,000
OBJ	20.87	19.98
F <sub>opt</sub> <sup>L</sup>	0.004	0.5474

The upper level design variables were taken at the end of the 15th cycle (using the response surface) and the set of thicknesses and areas that gives these upper level stiffnesses was found. No approximation was made here. Figure 7 shows the stiffness matching between the upper and lower levels; the response surface (shaded) is compared with the IADS formulation (black). The response surface design after 15 cycles matches the stiffness well ( $F_{opt}^L = 0.004$ ). The IADS design matches the stiffnesses poorly ( $F_{opt}^L = 0.5474$ ). These plots indicate that, although OBJ for the IADS procedure is smaller than that found by the response surface procedure, the design is infeasible because of poor matching, particularly in the flapwise bending and torsional stiffnesses. The response surface design, nevertheless, still violates the coordination constraint, which states that the matching must be within 0.001 ( $\gamma$ ).





**Figure 7. Stiffness Matching After 15 Cycles**

For the next 15 cycles, the move limits in the IADS formulation were cut in half in order to improve the results. Table 4 shows the optimization results after 30 cycles. Stiffness matching at the end of the 30th cycle is shown in Fig. 8. As seen in the plots, the matching of the IADS procedure has improved only slightly; the result remains an infeasible design. The smaller move limits, therefore, had little effect on the performance of the IADS procedure. On the other hand, for the response surface the matching has improved and  $F_{opt}^L$  has decreased to 0.0005; thus this design is feasible.

Table 4. Optimization Results after 30 Cycles

Upper Level Design Variable	Response Surface	IADS
Twist (deg)	-10.55	-11.65
Chord (ft)	0.4328	0.3504
$EI_{xx}$ (lb-ft <sup>2</sup> )	2,826	2,800
$EI_{zz}$ (lb-ft <sup>2</sup> )	210.5	214.3
GJ (lb-ft <sup>2</sup> )	228.0	228.0
EA (lb)	1,470,000	1,525,000
OBJ	20.73	19.93
$F_{opt}^L$	0.0005	0.6328

 Response surface formulation  
 IADS formulation

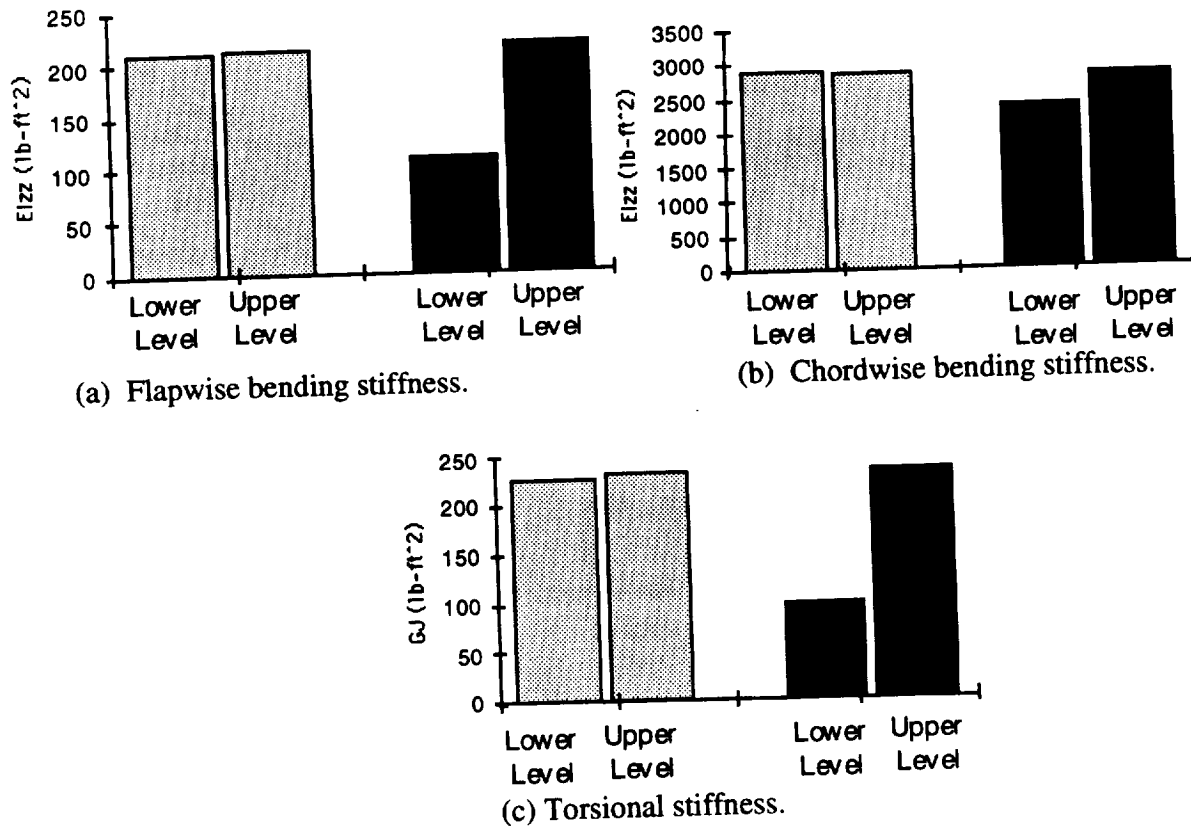


Figure 8. Stiffness matching after 30 cycles.

Because a change in the move limits for the IADS formulation resulted in no apparent improvement in the optimization, it was decided to use the original coordination constraint (Eq. (4)) used in Reference 6. This formulation has previously given good results; thus, it provides a fair comparison to the response surface results. The original optimization was repeated for the first 15 cycles; these results are shown in Fig. 9 and Table 5. From these plots, the IADS coordination has improved significantly, but the torsional stiffness again does not match well, so that the design is infeasible. However, these IADS results are similar to those obtained with the response surface.

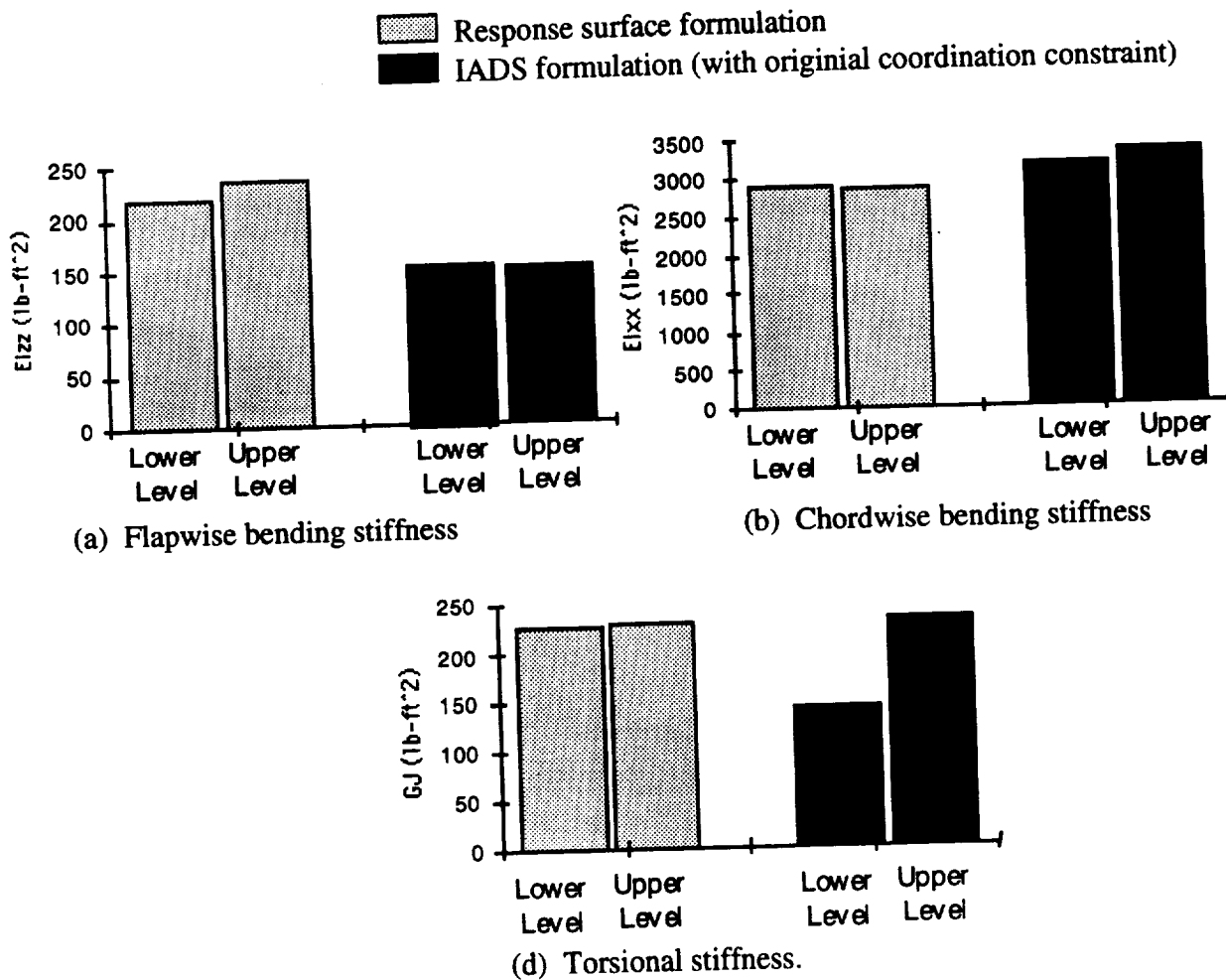


Figure 9. Stiffness matching After 15 cycles



Table 5. Optimization Results After 30 Cycles  
(IADS formulation uses original coordination constraint, Eqn. 4)

Upper Level Design Variables	Response Surface	IADS
Twist (deg)	-12.10	-11.49
Chord (ft)	0.4381	0.3836
El <sub>xx</sub> (lb-ft <sup>2</sup> )	2,831	3,011
El <sub>zz</sub> (lb-ft <sup>2</sup> )	231.9	163.0
GJ (lb-ft <sup>2</sup> )	225.4	253.3
EA (lb)	1,469,000	1,482,000
OBJ	20.67	20.23

Next the response formulation and the IADS formulation are examined on the basis of the number of structural optimizations required. In building the response surface, 127 structural optimizations were performed (one for each design point of the central composite design plus the 50 random points for validation). In the IADS formulation, a total of seven structural optimizations are conducted for each cycle: one for the lower level optimization and six for sensitivity analysis needed at the upper level. After 15 cycles, the IADS requires 105 structural optimizations and the response surface requires 127 optimizations. (Note: an additional structural optimization would be required in the response formulation to determine the structural thicknesses.) This indicates that the response surface formulation requires more structural optimizations after 15 cycles than the IADS formulation requires. However, the response formulation design is much better at this point than the IADS design. The stiffnesses match well for the response surface design and poorly for the IADS design. After 30 cycles, the IADS requires an additional 105 structural optimizations and the response formulation requires no additional structural optimizations. The IADS formulation still has poor stiffness matching. The response surface formulation continues to match the stiffnesses well. In Ref. 16 the IADS typically required more than 50 cycles to converge. The response surface formulation was allowed to run for additional cycles and the upper level objective continued to improve. When an actual structural optimization was done to obtain the stiffness matching, the matching was good. For the work presented, the response surface only needed to be generated once. The preliminary results of this research are encouraging and support the notion that response surfaces are a viable means of easing the difficulties associated with multidisciplinary design optimization. The response surface formulation can be used to arrive quickly at a viable design region and then the IADS procedure can be used to get a detailed design.

### Concluding Remarks

A response surface has been developed to replace the lower level structural optimization of a multilevel optimization procedure. During the course of this research, several important considerations were identified that must be addressed in the application of a response surface to this type of problem. The first consideration is to decide what the response surface will approximate and develop a measure of how well it will achieve this goal. In addition the coordination between the upper level and the response

surface must be appropriate. Finally, in replacing an entire structural optimization procedure with a response surface, the designs used to generate the surface must truly be optimal. The preliminary results presented in this paper are encouraging and confirm that response surfaces can be a viable way of easing the computational demands of multidisciplinary design optimization.

*Acknowledgements* - The research of the first author was partially supported under the Langley Aerospace Research Summer Scholars(LARSS) Program at NASA Langley Research Center in Hampton, Virginia.

## References

1. Sobieszczanski-Sobieski, J., "A Linear Decomposition Method for Large Optimization Problems-Blueprint for Development," NASA TM-83248, 1982.
2. Sobieszczanski-Sobieski, J., James, B. B., and Dovi, A. R., "Structural Optimization by Generalized, Multilevel Optimization," *AIAA J.*, Vol. 23, (11), November 1985.
3. Sobieszczanski-Sobieski, J., "Two Alternative Ways for Solving the Coordination Problem in Multilevel Optimization," NASA TM-104036, 1991.
4. Barthelemy, J.-F. M., "Engineering Applications of Multilevel Optimization Methods," Computer Aided Optimum Design of Structures, Proceedings of the 1st International Conference, Southampton UK, June 1989.
5. Wrenn G. A. , and Dovi, A. R., "Multilevel Decomposition Approach to the Preliminary Sizing of a Transport Aircraft Wing," *AIAA Journal of Aircraft*, Vol. 25, No. 7, July 1988, pp 632-638.
6. Zeiler, T. A., and Gilbert, M. G., "Integrated Control/Structure Optimization by Multilevel Decomposition," AIAA Paper No. 90-1057, AIAA/ASME/ASCE/AHS/ASC 31st Structures, Structural Dynamics and Materials Conference, Long Beach, California, April 2-4, 1990.
7. Barthelemy, J.-F. M., and Haftka, R. T., "Approximation Concepts for Optimum Structural Design - A Review," *Structural Optimization*, Vol 5, pp. 124-144, 1993.
8. Free, J. W., Parkinson, A. R., Bryce, G. R. , and Balling, R. J., "Approximation of Computationally Expensive and Noisy Functions for Constrained Nonlinear Optimization," ASME Design Engineering Technical Conference, Paper No. 86-DET-116, Columbus, Ohio, Oct. 5-8, 1986.
9. Eason, E. D., and Fenton, R. G. "A Comparison of Numerical Optimization Methods for Engineering Design." *ASME Journal of Engineering for Industry*, 96, 196-200 (1974).
10. White, K. P., Jr., Gabler, H. C., III, and Pilkey, W. D., "Approximating dynamic Response in Small Arrays Using Polynomial Parameterizations and Response Surface Methodology," *The Shock and Vibration Bulletin* , 55, pp. 167-173.

11. White, K. P., Jr., Howell, W. T., Gabler, H. C., III, and Pilkey, W. D., " Simulation Optimization of the Crashworthiness of a Passenger Vehicle in Frontal Collisions using Response surface Methodology," SAE International Congress and Exposition, Detroit, Michigan, Feb 25- Mar 1, 1985.
12. Toropov, V. V., "Simulation Approach to Structural Optimization," *Structural Optimization*, Vol 1, pp. 37-46, 1989.
13. Shoofs, A. J. G., "Experimental Design and Structural Optimization," Technical University of Eindhoven, Ph. D. Dissertation.
14. Carpenter, W. C., "Effect of Design Selection on Response Surface Performance," NASA CR-4520, June 1993.
15. Cornell, J. A., "How to Apply Response Surface Methodology, American Society for Quality Control, Statistics Division," Vol 8, 1990.
16. Walsh, J. L., Young, K. C., Pritchard, J. I., Adelman, H. M., and Mantay, W. R., "Multilevel Decomposition Approach to Integrated Aerodynamic/Dynamic/Structural Optimization of Helicopter Rotor Blades," NASA TM-109084, May 1994.
17. Vanderplaats, G. N., "CONMIN- A FORTRAN Program for Constrained Function Minimization, User's Manual," NASA TM X-62282, 1973.
18. Gessow, A., and Myers, G. C., Jr., Aerodynamics of the Helicopter. MacMillan Co., 1952  
Republished by Frederick Ungar Publ. Co., 1967.
19. Johnson, W., "A Comprehensive Analytical Model of Rotorcraft Aerodynamics and Dynamics – Johnson Aeronautics Version," Volume II, Users's Manual. CAMRAD/JA, Johnson Aeronautics (Palo Alto, California), 1988.
20. Kreisselmeir, G., and Steinhauser, R., "Systematic Control Design by Optimizing a Vector Performance Index," *Computer Aided Design on Control Systems*, W. A. Cuenod, ed., Pergamon Press, 1980, pp.113-117.





